Journal of Materials Chemistry

Cite this: *J. Mater. Chem.*, 2011, **21**, 5464

www.rsc.org/materials

PAPER

Functionalization of magnetic nanoparticles with peptide dendrimers

Rong Zhu,† Wen Jiang,† Yuji Pu, Kui Luo, Yao Wu,* Bin He and Zhongwei Gu*

Received 20th August 2010, Accepted 2nd February 2011
DOI: 10.1039/c0jm02752a

Surface functionalization of magnetic nanoparticles (MNPs) has been an exciting area of interest for researchers in biomedicine. In this paper, we introduce a new family of peptide dendritic ligands for functionalizing MNPs of superior quality. L-Lysine- and L-glutamic acid-based dendritic ligands with dopamine located at the focal points were fully designed and synthesized before the functionalization. Then ligands of different dendritic generations (**G1** to **G3**) were immobilized on the surface of oleic-acid-coated hydrophobic MNPs *via* ligand-exchange method to realize phase transfer. The two series of modified MNPs were systematically studied *via* FTIR, TGA, XRD, TEM, DLS, VSM and zeta potential measurements. The modified MNPs exhibited an adjustable number of terminal functional groups and superior stability in aqueous solutions in a broad pH range. The surface existence of water-soluble polypeptide ligands promoted monodispersity of the particles and led to an increased hydrodynamic diameter under 30 nm from **G1** to **G3**. After the ligand exchange process, the superparamagnetic behavior was successfully retained. The two series of modified MNPs exhibited approximate magnetization in the same generation, while the saturation magnetization of the MNPs decreased with increasing surface dendritic generation. MNPs functionalized with **G1** L-glutamic acid dendritic ligands had the highest saturation magnetization (55 emu g^{-1}), which was larger than for the initial MNPs. This novel functionalization strategy provides a potential platform for designing and preparing highly stable ultrafine MNPs with high magnetization for biomedicinal applications.

Introduction

Magnetic nanoparticles (MNPs) have attracted more and more attention for their wide range of biomedical applications, such as targeted drug delivery,[1–3] contrast agents in magnetic resonance imaging (MRI),[3–5] hyperthermia treatment,[6] gene carriers[7] and protein separation.[8,9] Properties of MNPs that are required for these biomedical applications are high magnetization value,[10] monodispersity and narrow size distribution, good stability and biocompatibility.[11,12] The thermal decomposition method is commonly regarded as the best way to produce high quality ultrafine monodisperse MNPs with controllable size less than 20 nm.[13–15] However, owing to the long-chain alkane ligands on the surface, the obtained MNPs are hydrophobic and only disperse in nonpolar or weakly polar solvents, such as *n*-hexane or chloroform. The hydrophobicity significantly restricts their biological applications *in vivo*.

Surface hydrophilic functionalization has been used to modify MNPs, leading to good dispersibility and stability in aqueous solution.[16] Two strategies, known as surface encapsulation[17] and ligand-exchange, are commonly carried out to prepare hydrophilic MNPs. The surface encapsulation often utilizes amphiphilic polymer to form micelle-like double-layer structures outside the hydrophobic nanoparticles.[18] It has the advantage for large-scale preparation of hydrophilic MNPs. However, there are several bottlenecks for this approach. First, the obtained MNPs cannot be stable under physiological conditions because of the weak interaction between hydrophobic double-layer structures.[19] Second, the size of the amphiphilic copolymer-encapsulated MNPs often exceeds 30 nm,[19–21] and this would result in shorter blood circulation time *in vivo*.[22] Furthermore, it is very difficult to manipulate the number of terminal functionalities for controllable bioconjugation due to the uncertainty in the number functional groups in polymer.

Ligand-exchange is a novel method whereby the original ligands on the surface can be displaced without changing the intrinsic properties of the iron core. Compared with surface-encapsulation, the MNPs resulting from this approach are more stable because they form stronger coordinate bonds during the surfactant exchange reaction,[18] which overcomes the inherent shortcomings of the surface-encapsulated MNPs. Polyelectrolyte-[23] and PEG-based hydrophilic polymers have been employed to prepare hydrophilic MNPs by the ligand-exchange approach.[24–26] These linear polymers can preserve agglomeration and minimize protein adsorption, but it is difficult to control the final size of the phase-transformed MNPs to be within the desired range.[27,28]

National Engineering Research Center for Biomaterials, Sichuan University, Chengdu, 610064, People's Republic of China. E-mail: zwgu@scu.edu.cn; Fax: +86 28-85410653; Tel: +86 28-85414308; wuyao@scu.edu.cn; +86 28-85410653; +86 28-85410336
† These authors contributed equally to this work.

Recently, dendritic macromolecules have been investigated as ligands for surface modification of MNPs.[29,30] The dendritic ligands are multivalent macromolecules which possess highly controlled structure, such as a single molecular weight, a large number of controllable "peripheral" functionalities and nanoscopic dimensions. PAMAM dendrimers and their derivatives are classic examples in the modification of core–shell-type nanoparticles.[7,25,31] However, recent studies have shown that PAMAM dendrimers are cytotoxic, particularly in the higher generations of protonated (cationic) dendrimers with large numbers of amine groups,[32–34] which limits their biomedical applications. Polypeptide dendrimers are considered as new biomaterials due to their protein-like structures, multivalence, excellent biocompatibility, degradability and low immunogenicity.[35,36] In the previous research of our group, peptide dendrimers were synthesized successfully as MRI probes, gene delivery and drug delivery carriers with excellent biocompatibility and good results.[37–40]

In this work, we demonstrate the feasibility of functionalizing hydrophobic ultrafine MNPs with a new family of peptide dendrimers through the ligand-exchange method for the first time. Different from the PAMAM-grafted method, L-lysine- and L-glutamic acid-based dendritic ligands of different generations with dopamine located at the focal point have been synthesized before grafting onto the MNP surface. It is beneficial to precisely control the terminal functional groups and reduce the sizes of phase-transferred MNPs to be less than 30 nm. We systematically compare the performance of the functionalized MNPs with the initial oleic-acid-coated particles in terms of the surface functional groups coverage, crystalline structure, size distribution, magnetic properties and surface charge at different pH values.

Experimental methods

Materials

Iron(III) acetylacetonate, phenyl ether, benzyl ether, oleic acid (OA) (90%), oleylamine (>70%), 1,2-hexadecanediol (90%), trifluoroacetic acid (TFA) and *N*,*N*-diisopropylethylamine (DIPEA) were purchased from Sigma-Aldrich and used as received. N_{α}, N_{ϵ}-di-Boc-L-lysine(Boc-Lys(Boc)-OH), *O*-benzotriazole-*N*,*N*,*N*′,*N*′-tetramethyluromium hexafluorophosphate (HBTU), 1-hydroxybenzotriazole (HOBt) were purchased from GL Biochem (Shanghai) Ltd. and used as received.

Characterization methods

Characterization and structural confirmation of the dendritic intermediates and products were performed by NMR, electrospray ionization time-of-flight mass spectrometry (ESI-MS) and matrix assisted laser desorption ionization time-of-flight mass spectrometry (MALDI-TOF MS). NMR data were obtained using a 400 MHz Bruker Advance 400 spectrometer, and chemical shifts were reported in ppm on the δ scale relative to TMS or solvent. Electrospray mass spectra using an electrospray ionization mode were obtained using a Waters Q-TOF Premier time-of-flight mass spectrometer operated in positive or negative ion mode. MALDI-TOF analysis of modified dendritic macromolecules was performed on Autoflex MALDI-TOF/TOF.

Fourier transform infrared (FTIR) spectra were performed on PE spectrometer. The spectra were recorded in the wave number interval between 4000 and 400 cm^{-1} with step length 4 cm^{-1}. The samples were compressed into KBr pellets for the measurements. Thermal gravimetric analysis (TGA) was performed on STA 449 C Jupiter (NETZSCH). The mass loss of the dried sample was monitored under N_2 at temperatures from 35 °C to 1000 °C with a heating rate of 10 K min^{-1}. The crystal structure of the iron oxide nanoparticles was tested by powder X-ray diffraction (XRD) pattern with angles ranging from 20° to 90° (Philips). The transmission electron microscopy (TEM) was carried out on a JEOL JEM-2010F instrument (Japan Electronic). Samples were prepared by deposition of one drop of an appropriately diluted solution onto a copper grid and dried at ambient temperature before they were loaded into the microscope. Dynamic light scattering (DLS) and zeta potential were measured by a Malvern Nano-ZS instrument. The samples were dispersed in *n*-hexane or Milli-Q water in glass cuvettes and tested at 25 °C for the size characterization. The magnetization of the dried sample was measured by a vibrating sample magnetometer (VSM, Model BHV-525, Riken Japanese Electronics Company) with field up from 0 to 15000 Oe at 300 K. The zeta potentials were recorded in a solution of functionalized MNPs in water with pH ranging from 2 to 12. The pH values were adjusted by 10 mM HCl and 10 mM NaOH solution.

Synthesis of magnetite nanoparticles (MNPs-OA)

Fe_3O_4 nanoparticles were prepared according to the method reported by Sun *et al.*[13] Briefly, $Fe(acac)_3$ (2.0 mmol), 1,2-hexadecanediol (10.0 mmol), oleylamine (6.0 mmol) and oleic acid (6.0 mmol) were dissolved in a solution of 20 mL benzyl ether. The solution was heated at 200 °C for 2 h, refluxed at 300 °C for 1 h, and then cooled to room temperature. The black particles were precipitated with ethanol and collected by centrifugation at 8000 rpm for 10 min, reprecipitated and washed with ethanol 3 times. The product was then re-dispersed in *n*-hexane.

Synthesis of polypeptide dendritic ligands

L-Lysine-based dendritic macromolecules with Boc protection groups were synthesized by divergent and convergent approaches, as shown in Scheme 1. L-Glutamic acid-based dendritic macromolecules with benzyl protection groups were synthesized by a convergent approach (Scheme 2). Compounds **1**,[41] **7**,[41] **5**,[42] **9**[43] were prepared according to the literature. The synthesis of other compounds is described below.

Compound 2. Compound **1** (0.5 g, 1.2 mmol) was treated with 5% TFA in dichloromethane (CH_2Cl_2, 30 mL) at room temperature for 5 h. The solvent was removed under vacuum to give an oil, and 40 mL of ethyl ether was added. The mixture was stirred overnight. The white solid was collected by centrifugation. The product was used without further purification. The solid was dissolved in 10 mL DMF. DIPEA (1.7 mL, 10.4 mmol) was added to the mixture, followed with N_{α},N_{β}-di-Boc-L-lysine (479.0 mg, 1.2 mmol). The solution was stirred under nitrogen atmosphere for 10 min and cooled to 0 °C. HBTU (0.455 g, 1.2 mmol) and HOBt (0.163 g, 1.2 mmol) were added to the

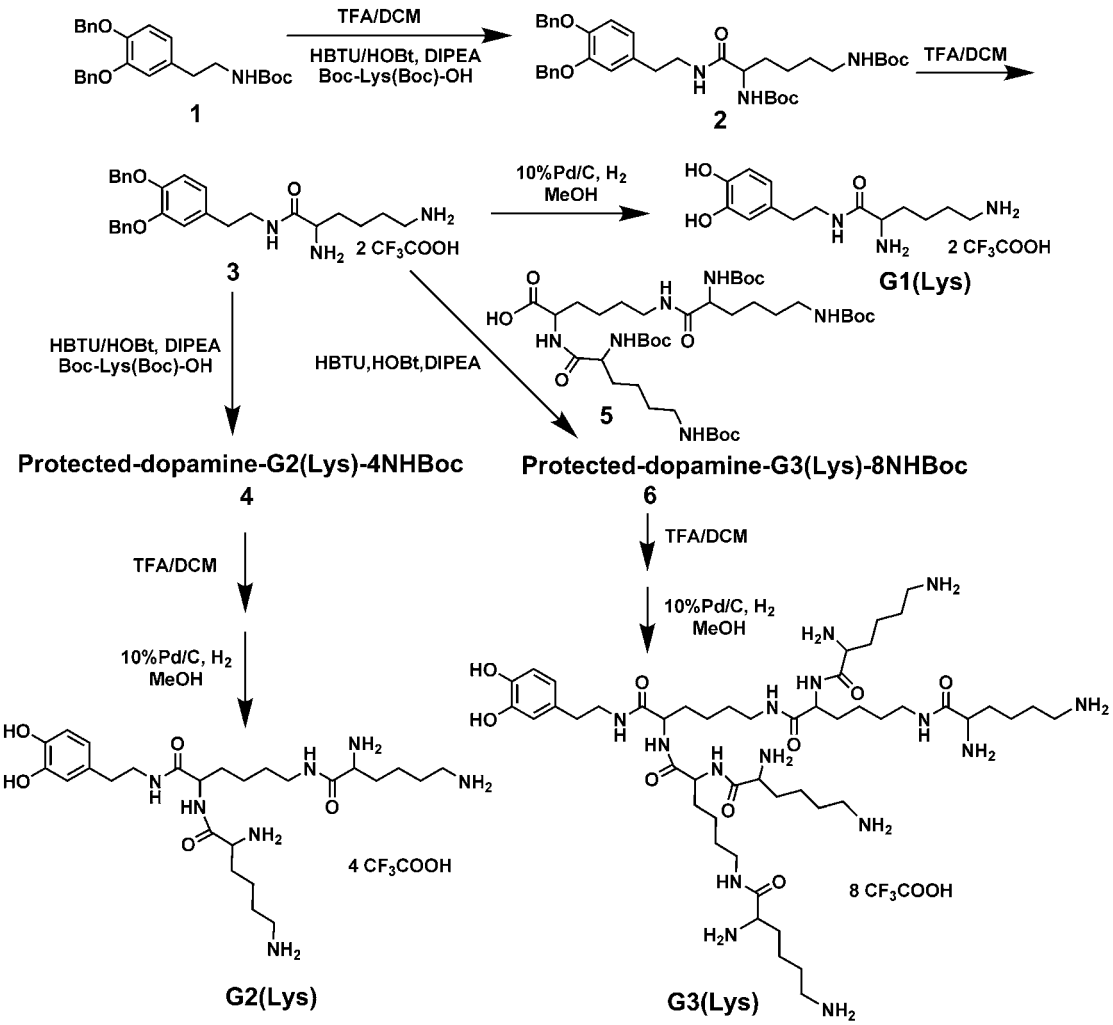

Scheme 1 The synthesis of different generations of L-lysine-based dendritic ligands.

solution. The solution was stirred at room temperature for 24 h. Ethyl acetate (EtOAc, 150 mL) was added, the organic solution was washed with saturated $NaHCO_3$, $NaHSO_4$ (0.1 M), saturated $NaHCO_3$ and brine. The organic phase was dried by anhydrous Na_2SO_4, filtered, and the solvent was removed under reduced pressure. The crude product was purified by column chromatography (silica gel, $CHCl_3$–CH_3OH = 10 : 1) to give compound **2** as a white solid. Yield = 83.0% (0.56 g, 1.0 mmol). ^{1}H NMR (400 MHz, $CDCl_3$): δ 7.48–7.27 (m, 10H, C_6H_5), 6.88–6.80 (m, 2H, dopamine aromatics), 6.70 (d, *J* 8.0, 1H, dopamine aromatics), 6.07 (s, 1H, N*H*), 5.15–5.13 (m, 4H, benzyl CH_2), 5.04 (s, 1H, N*H*), 4.54 (m, 1H, COC*H*(CH_2)NH), 3.95 (m, 1H, N*H*), 3.44 (m, 2H, NHC$H_2$$CH_2$–Ar), 3.07 (m, 2H, COCH(CH_2)NH), 2.72 (t, 2H, NHCH$_2$CH_2-Ar), 1.88–1.18 (m, 18H, (CH_3)$_3$C- and 6H, CH_2); ^{13}C NMR (100 MHz, $CDCl_3$): δ (100 MHz, $CDCl_3$) 172.03 (*C*ONH), 156.16, 155.74 (*C*OOC(CH_3)$_3$), 149.08–137.40 (dopamine aromatics), 132.14–115.40 (C_6H_5), 79.96–79.10 (O*C*(CH_3)$_3$), 71.45–71.32 (benzyl *C*H$_2$), 54.50 (CO*C*H(R)NH), 53.45 (CO*C*H(R)NH), 40.98–38.38 (*C*H$_2$NH), 35.31 (*C*H$_2$–C_6H_5), 31.15, 29.70, 29.59 (OC(*C*H$_3$)$_3$), 28.01, 27.59, 27.55, 22.95, 22.80, 22.41 (all *C*H$_2$); ESI-TOF MS: *m*/*z* = 662.38 (M + H$^+$) (calculated 661.83 for $C_{38}H_{51}N_3O_7$).

Compound 4 (Protected-dopamine-G2(Lys)-4NHBoc). The Boc group on dendritic compound **2** (0.56 g, 0.85 mmol) was removed by the same procedure as described in the synthesis of dendritic compound **2**. The deprotected compound was dissolved in 10 mL DMF. DIPEA (1.3 mL, 7.61 mmol) and N_α,N_β-di-Boc-L-lysine (0.733 g, 2.12 mmol) were added. The solution was stirred under nitrogen atmosphere for 10 min and cooled to 0 °C. HBTU (802 mg, 2.1 mmol) and HOBt (288 mg, 2.1 mmol) were added to the reaction system as a solid mixture. The solution was stirred for 48 h at room temperature. 150 mL EtOAc was added, the organic solution was washed with saturated $NaHCO_3$, $NaHSO_4$ (0.1 M), saturated $NaHCO_3$ and brine. The organic phase was dried by anhydrous Na_2SO_4, filtered, and the solvent was removed under reduced pressure. The product was purified by column chromatography (silica gel, $CHCl_3$–CH_3OH = 15 : 1) to yield compound **4** as a white solid. Yield = 83.0% (1.363 g, 0.60 mmol). ^{1}H NMR (400 MHz, $CDCl_3$): δ 7.52–7.28 (10H, m, C_6H_5), 7.15 (s, 1H, N*H*), 6.88–6.80 (m, 2H, dopamine aromatics), 6.70 (d, *J* 8.0, 1H, dopamine aromatics), 6.50 (s, 1H, N*H*), 5.90 (s, 1H, N*H*), 5.46 (s, 1H, N*H*), 5.15–5.13 (m, 4H, benzyl CH_2), 4.85 (s, 1H, N*H*), 4.76 (s, 1H, N*H*), 4.32–3.99 (m, 3H, COC*H*(CH_2)NH), 3.48 (m, 2H, NHC$H_2$$CH_2$–Ar),

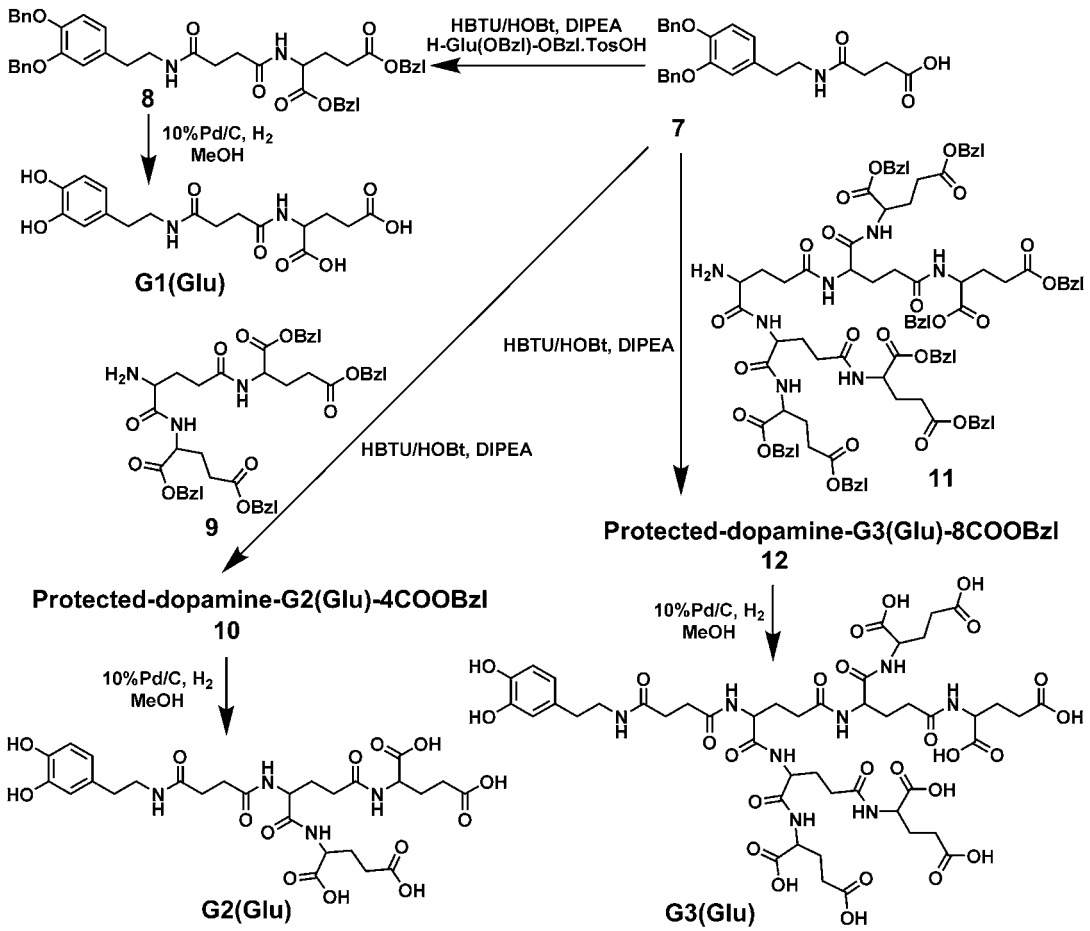

Scheme 2 The synthesis of different generations of L-glutamic acid dendritic ligands.

3.19–2.86 (m, 6H, COCH(CH_2)NH), 2.70 (m, 2H, NHCH_2CH_2-Ar), 1.98–1.07 (m, 36H, (CH_3)$_3$C- and 18H, CH_2); ^{13}C NMR (100 MHz, $CDCl_3$): δ 173.40, 171.78, 168.27 (*C*ONH), 156.38 (*C*OOC(CH$_3$)$_3$), 149.23, 147.77, 137.57, 137.46 (dopamine aromatics), 132.60, 128.79, 128.55, 128.40, 127.89, 127.86, 127.54, 127.46, 121.80, 116.02, 115.72 (C_6H_5), 80.19, 79.98, 79.09 (O*C*(CH$_3$)$_3$), 71.68, 71.49 (benzyl *C*H$_2$), 54.50, 54.39, 53.45 (CO*C*H(R)NH), 40.98, 40.32, 40.07, 38.38 (*C*H$_2$NH), 35.31 (*C*H$_2$–C_6H_5), 32.56, 32.16, 31.68, 31.15, 29.70, 29.59, 29.01, 28.59 (OC(*C*H$_3$)$_3$), 28.55, 22.95, 22.80, 22.41 (all *C*H$_2$); ESI-TOF MS: m/z = 1118.68 (M + H$^+$) (calculated 1117.67 for $C_{60}H_{91}N_7O_{13}$).

Compound 6 (Protected-dopamine-G3(Lys)-8NHBoc). The crude product **3** which was obtained from compound **2** (0.8 g, 1.21 mmol) as described before, was dissolved in 50 mL DMF. DIPEA (3.7 mL, 22.17 mmol) and compound **5** (2.17 g, 2.46 mmol) were added to the mixture. The solution was stirred under nitrogen atmosphere for 10 min and cooled to 0 °C. HBTU (933 mg, 2.46 mmol) and HOBt (335 mg, 2.46 mmol) were added to the solution as a solid mixture. Subsequently, the reaction mixture was stirred at room temperature for 48 h. The solvent was removed by rotary evaporation and the residue was dissolved in 100 mL of EtOAc and washed with saturated $NaHCO_3$, $NaHSO_4$ (0.1 M), saturated $NaHCO_3$ and brine. The organic phase was dried by anhydrous Na_2SO_4, filtered, and the solvent was removed under reduced pressure. The product was purified by column chromatography (silica gel, $CHCl_3$–EtOAc–CH_3CH_2OH = 6 : 2 : 1) to yield compound **6** as a white solid. Yield = 40% (0.98 g, 0.48 mmol). ^{1}H NMR (400 MHz, $CDCl_3$): δ 7.78 (s, 1H, N*H*), 7.74 (m, 2H, N*H*), 7.51–7.27 (m, 10H, C_6H_5), 6.88–6.80 (m, 2H, dopamine aromatics), 6.70 (d, J 8.0, 1H, dopamine aromatics), 6.06 (s, 1H, N*H*), 5.75 (s, 1H, N*H*), 5.60 (m, 2H, N*H*), 5.15–5.13 (m, 4H, benzyl CH_2), 4.62–4.01(m, 7H, COC*H*(CH$_2$)NH), 3.43 (m, 2H, NHCH_2CH$_2$–Ar), 3.34–2.82 (m, 14H, COCH(CH_2)NH), 2.69 (m, 2H, NHCH$_2$CH_2-Ar), 1.96–1.00 (m, 72H, (CH_3)$_3$C- and 42H, CH_2); ^{13}C NMR (100 MHz, $CDCl_3$): δ 177.43, 173.76, 173.36, 173.05, 173.03, 172.94, 172.24, 171.76, 168.03 (*C*ONH), 158.63, 156.58 (*C*OOC(CH$_3$)$_3$), 149.29, 147.86, 147.24, 137.57 (dopamine aromatics), 132.65, 131.22, 130.17, 129.13, 128.97, 128.75, 128.59, 128.11, 127.73, 127.64, 121.96, 116.07, 115.72 (C_6H_5), 80.51–79.28 (O*C*(CH$_3$)$_3$), 71.79, 71.65 (benzyl *C*H$_2$), 68.44, 65.86 (O*C*(CH$_3$)$_3$), 55.37, 54.82, 54.52, 54.28, 53.50, 53.35 (CO*C*H(R)NH), 40.46, 40.25, 39.01 (*C*H$_2$NH), 35.36 (*C*H$_2$–C_6H_5), 32.22, 31.72, 30.85, 30.65, 30.45, 29.99, 29.65, 29.21, 28.76 (OC(*C*H$_3$)$_3$), 28.01, 27.50, 27.02, 24.03, 23.50, 23.28, 22.98 (all *C*H$_2$); MALDI-TOF MS: m/z = 2054.8 (M + Na$^+$) (calculated 2031.6 for $C_{104}H_{171}N_{15}O_{25}$).

Compound 8. Compound **7** (200 mg, 0.46 mmol) was dissolved in 20 mL DMF, H-Glu-(OBzl)$_2$·TosOH (230 mg, 0.46 mmol)

was added and the solution was cooled to 0 °C. DIPEA (0.5 mL, 2.76 mmol), HBTU (175 mg, 0.46 mmol) and HOBt (63 mg, 0.46 mmol) were added to the reaction system. The solution was stirred at room temperature for 24 h. The solvent was removed using a rotary evaporator and the residue was dissolved in 45 mL of EtOAc, and washed with saturated $NaHCO_3$, $NaHSO_4$ (0.1 M), saturated $NaHCO_3$ and brine. The organic phase was dried by anhydrous Na_2SO_4 and filtered. The solvent was removed under reduced pressure and further purified by column chromatography (silica gel, $CHCl_3$–CH_3OH = 10 : 1) to give compound **8** as a white solid. Yield = 73% (250 mg, 0.34 mmol). ^{1}H NMR (400 MHz, $CDCl_3$): δ 7.51–7.24 (m, 20H, C_6H_5), 6.88–6.77 (m, 2H, dopamine aromatics), 6.62 (d, *J* 8.0, 1H, dopamine aromatics), 5.72 (d, 1H, N*H*), 5.73 (s, 1H, N*H*), 5.26–5.00 (m, 8H, benzyl CH_2), 4.62 (m, 1H, C*H*), 3.38 (m, 2H, NHCH_2CH$_2$–Ar), 2.65 (t, 2H, NHCH$_2$CH_2-Ar), 2.56–1.60 (m, 4H, -COCH_2CH_2CO- and 2H, -CH$_2$CH_2CO- and 2H, -CHCH_2CH$_2$-); ^{13}C NMR (100 MHz, $CDCl_3$): δ 172.50, 172.24, 172.07, 171.85, 171.55 (*C*ONH), 148.96, 147.60, 137.37, 137.27, 135.68, 135.18 (dopamine aromatics), 132.27, 128.59, 128.54, 128.44, 128.27, 128.23, 127.76, 127.74, 127.33, 127.29, 126.93, 121.56, 115.68, 115.34 (C_6H$_5$), 71.39, 71.23, 67.22, 66.47 (benzyl *C*H$_2$), 51.73 (*C*H), 40.74, 35.05, 31.63, 31.45, 31.38, 30.16, 29.67, 27.09 (-CO*C*H$_2$*C*H$_2$CO-); ESI-TOF MS: *m*/*z* = 742.38 (M + H$^+$) (calculated 742.86 for $C_{45}H_{46}N_2O_8$).

Compound 10 (Protected-dopamine-G2(Glu)-4COOBzl). Compound **7** (280 mg, 0.65 mmol) was dissolved in 25 mL DMF, then DIPEA (0.6 mL, 3.87 mmol) and compound **9** (742 mg 0.97 mmol) were added to the mixture. The solution was stirred under nitrogen atmosphere for 10 min and cooled to 0 °C. HBTU (367 mg, 0.97 mmol) and HOBt (132 mg, 0.97 mmol) were added. The solution was stirred at room temperature for 24 h. The solvent was removed by rotary evaporation and the residue was dissolved in 50 mL of EtOAc and washed with saturated $NaHCO_3$, $NaHSO_4$ (0.1 M), saturated $NaHCO_3$ and brine. The organic phase was dried by anhydrous Na_2SO_4 and filtered, and the solvent was removed under reduced pressure. The crude product was purified by column chromatography (silica gel, $CHCl_3$–CH_3OH = 15 : 1) to yield compound **10** as a white solid. Yield = 55% (419 mg, 0.36 mmol). δ 7.85 (d, 1H, N*H*), 7.60–7.20 (m, 30H, C_6H_5), 6.88–6.76 (m, 2H, dopamine aromatics), 6.68 (d, *J* 8.0, 1H, dopamine aromatics), 5.27–4.94 (m, 12H, benzyl CH_2), 4.80–4.30 (m, 3H, C*H*), 3.37 (m, 2H, NHCH_2CH$_2$–Ar), 2.64 (t, *J* 7.2, 2H, NHCH$_2$CH_2-Ar), 2.54–1.62 (m, 4H, -COCH_2CH_2CO- and 6H, -CH$_2$CH_2CO- and 6H,-CHCH_2CH$_2$-); ^{13}C NMR (100 MHz, $CDCl_3$): δ 173.22, 172.96, 172.80, 172.34, 172.33, 171.94, 171.90, 171.68 (*C*ONH), 148.99, 147.61, 137.41, 137.30, 135.76, 135.67 (dopamine aromatics), 134.99, 134.94, 132.32, 128.62, 128.61, 128.57, 128.53, 128.49, 128.45, 128.31, 128.25, 128.23, 128.18, 127.77, 127.74, 127.36, 127.32, 121.61, 115.72, 115.39 (C_6H$_5$), 71.43, 71.26, 67.71, 67.63, 66.52, 66.42 (benzyl *C*H$_2$), 52.38, 51.72, 51.57 (*C*H), 40.71, 35.08, 32.04, 31.44, 31.34, 30.51, 30.29, 28.48, 26.68, 26.61 (-CO*C*H$_2$*C*H$_2$CO-); ESI-TOF MS: *m*/*z* = 1181.53 (M + H$^+$) (calculated 1180.50 for $C_{69}H_{72}N_4O_{14}$).

Compound 12 (Protected-dopamine-G3(Glu)-8COOBzl). Compound **7** (536 mg, 1.24 mmol) was dissolved in 25 mL DMF, then DIPEA (1.2 mL, 7.41 mmol) and compound **11** (2.03 g, 1.24 mmol) were added to the mixture. The solution was stirred under a nitrogen atmosphere for 10 min and cooled to 0 °C. HBTU (468 mg, 1.24 mmol) and HOBt (169 mg, 1.24 mmol) were added to the reaction system. The solution was stirred at room temperature for 24 h. The solvent was removed by rotary evaporation and the residue was dissolved in 60 mL of EtOAc and washed with saturated $NaHCO_3$, 10% $NaHSO_4$, saturated $NaHCO_3$ and brine. The organic phase was dried by anhydrous Na_2SO_4, and filtered. The solvent was removed under reduced pressure. The crude product was purified by column chromatography (silica gel, $CHCl_3$–EtOAc–CH_3CH_2OH = 6 : 2 : 1) to yield compound **12** as a white solid. Yield = 32.2% (819 mg, 0.4 mmol). ^{1}H NMR (400 MHz, $CDCl_3$): δ 8.53 (s, 1H, N*H*), 8.23–8.08 (m, 2H, N*H*), 7.94 (m, 2H, N*H*), 7.73 (d, *J* 8.8, 1H, N*H*), 7.62 (d, 2H, N*H*), 7.54–7.16 (m, 50H, C_6H_5), 6.85–6.79 (m, 2H, dopamine aromatics), 6.68 (d, *J* 8.0, 1H, dopamine aromatics), 5.23–4.89 (m, 20H, benzyl CH_2), 4.78–4.13 (m, 7H, C*H*), 3.34 (m, 2H, NHCH_2CH$_2$–Ar), 2.64 (t, *J* 7.2, 2H, NHCH$_2$CH_2-Ar), 2.58–1.50 (m, 4H, -COCH_2CH_2CO- and 14H, -CH$_2$CH_2CO- and 14H, -CHCH_2CH$_2$-); ^{13}C NMR (100 MHz, $CDCl_3$): δ 173.09, 172.89, 172.77, 172.53, 172.42, 172.12, 171.95, 171.76, 171.66, 171.36 (*C*ONH), 148.77, 147.18, 137.96, 137.85, 136.78, 136.57 (dopamine aromatics), 136.36, 136.36, 136.28, 135.73, 128.86, 128.78, 128.48, 128.48, 128.43, 128.32, 128.25, 128.21, 128.21, 128.00, 127.89, 121.60, 116.01, 115.60, 115.25 (C_6H$_5$), 70.78, 70.66, 66.52, 66.41, 65.99 (benzyl *C*H$_2$), 51.93, 51.84, 51.76, 51.52, 51.31 (*C*H), 40.71, 36.67, 35.20, 35.16, 33.40, 32.08, 32.06, 30.31, 30.14, 26.49, 26.40 (-CO*C*H$_2$*C*H$_2$CO-); MALDI-TOF MS: *m*/*z* = 2081.9 (M + Na$^+$) (calculated 2058.3 for $C_{117}H_{124}N_8O_{26}$).

Ligands of Gn(Lys) and G*n*(Glu) (*n* = 1, 2, 3)

100 mg (0.15 mmol) of compound **2** were added in the mixture of CH_2Cl_2 (1 mL) and TFA (1 mL). The solvent was removed. The yellow oil residue was dissolved in MeOH, and 10% Pd/C (50 mg) was added. The resulting mixture was stirred under H_2 (50 pis) for 24 h. The Pd/C was filtered, and the filtrate was removed in vacuum to yield **G1(Lys)** as a white solid. Yield = 98%. ^{1}H NMR analysis showed that both the Bn and *t*-Boc protecting groups were removed from the dendritic molecules. This compound was used without further purification.

Dendritic ligands **G2(Lys)**, **G3(Lys)**, **G1(Glu)**, **G2(Glu)** and **G3 (Glu)** were synthesized with the same procedure as described in synthesis of **G1(Lys)**.

Preparation of MNPs functionalized with peptide dendrimers

The solid **G1(Lys)** (100 mg) was dissolved in a mixture of MeOH (40 mL) and $CHCl_3$ (20 mL), and the **MNPs-OA** in *n*-hexane (5 mL, 10 mg mL^{-1}) were introduced and shaken overnight to facilitate ligand-exchange. The solvent was removed under reduced pressure. The dendritic ligands modified MNPs were precipitated in *n*-hexane and collected by centrifugation at 3500 rpm. After washing with *n*-hexane (30 mL) 3 times, the product was re-dispersed in distilled water. The extra surfactants and salts were removed by dialysis using a dialysis bag (MWCO = 8000–14000) for 24 h in water to give **MNPs-G1(Lys)**. The

MNPs-G2(Lys), **MNPs-G3(Lys)**, **MNPs-G1(Glu)**, **MNPs-G2(Glu)** and **MNPs-G3(Glu)** were synthesized similarly.

Results and discussion

Synthesis of dendritic ligands and surface-modified MNPs

In order to form a stable surface coating, various surface binding groups have been explored in the past, such as carboxylate (COO^-),[44,45] phosphate (PO_3^{3-}),[29] and alcohol (OH^-).[46] Recent work has showed that bidentate ligands, such as dopamine,[24,41,47] exhibited high affinity to the MNP surfaces and could replace the capping ligands, oleic acid and oleyl amine. Therefore, we utilized dopamine as a robust anchor to conjugate peptide dendrimers with MNPs, as shown in Scheme 1–3. Polypeptide dendrimers were synthesized through divergent and convergent approach, and fully characterized by ^1H NMR, ^{13}C NMR, ESI-TOF MS and MALDI-TOF MS. In the MALDI-TOF mass spectrum of ligand **12** ($M = 2058.27$), the most abundant peak is observed at $m/z = 2081.9$ and 2097.7, which correspond to the $[M + Na]^+$ and $[M + K]^+$ signals, respectively, indicating that the designed third-generation dendritic ligand with dopamine located at the focal point has been successfully synthesized (Fig. 1).

Moreover, the ligand-exchange reaction has been optimized from typical procedures, involving the solvent used in the grafting experiments and the amount of dendritic ligands coated on the MNPs. In a typical grafting and phase transfer procedure, DMF or aqueous solution was usually used. In order to make the solution homogeneous, three solvents (CH_3OH, $CHCl_3$ and *n*-hexane) were introduced in our system. In such a medium, all

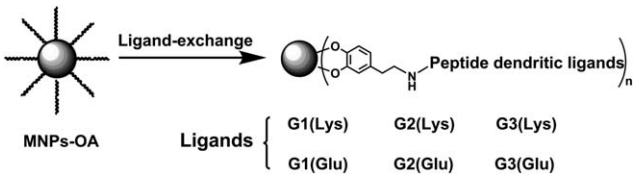

Scheme 3 The schematic route to MNPs unctionalized with peptide dendrimers.

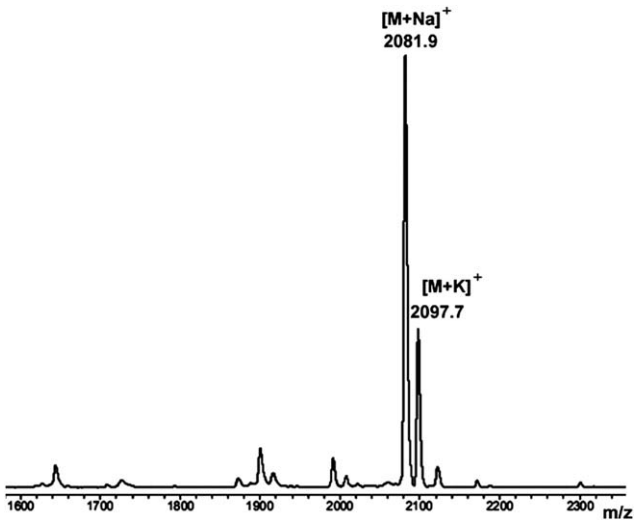

Fig. 1 The MALDI-TOF MS spectra of dendritic ligand **12**.

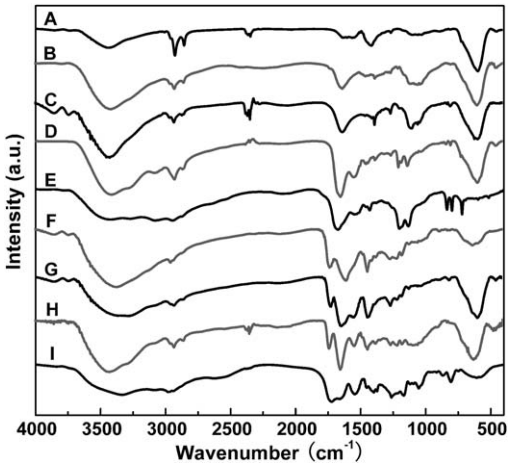

Fig. 2 FTIR spectra of the MNPs: (A) MNPs-OA; (B) MNPs-G1(Lys); (C) MNPs-G2(Lys); (D) MNPs-G3(Lys); (E) G3(Lys); (F) MNPs-G1(Glu); (G) MNPs-G2(Glu); (H) MNPs-G3(Glu); (I) G3(Glu).

the particles remained in a colloidal state. It presumed that a generally good integrity of polymer shell on the nanoparticles was obtained during the ligand-exchange reaction.[48]

Surface coverage and functional groups of the modified MNPs

The surface properties of the MNPs modified with peptide dendrimers were confirmed by FTIR spectra as shown in Fig. 2. The oleic-acid-coated MNPs (Fig. 2A) showed strong bands at 2922 and 2852 cm^{-1}, which are known as the characteristic peaks of CH_2 chain in oleic acid. Alkene stretches at 3009 and 1638 cm^{-1}, and two carboxylate stretches at 1538 and 1415 cm^{-1} further confirmed that oleic acid was chemisorbed on the surface of the nanoparticles.[49] After the ligand-exchange reaction, several differences were observed in the spectra. In the series of L-lysine-based dendrimers functionalized MNPs (Fig. 2B–D), the bands at 3200–3600 cm^{-1} were attributed to the bending vibration of the $–NH_2$ group. The strength of $–CH_2$ stretching at around 2922 and 2852 cm^{-1} dramatically decreased compared with the initial MNPs, indicating the disappearance of oleic acid. However, Fig. 2B–D showed that the bands at 2922–2931 cm^{-1} greatly increased with increasing dendritic generation, due to the different number of alkane chains in polypeptide dendrimers. Compared with FTIR spectra of lysine-based dendrimers, such as **G3(Lys)** (Fig. 2E), two prominent bands at 1650 and 1547 cm^{-1} were observed in the corresponding modified MNPs (Fig. 2B–D), which was attributed to the presence of –CO–NH– bands. A characteristic C–N peak was observed at about 1130 cm^{-1}. The strong bands at about 600 cm^{-1} were the Fe–O vibrations related to the ferrite core.[49] The results indicated that oleic acid was successfully replaced by lysine-based dendritic ligands.

In another series of MNPs modified with L-glutamic acid dendrimers (Fig. 2F–H), the O–H stretching frequency appeared in the range 3200–3600 cm^{-1}. Similar to the L-lysine-based series in Fig. 2B–D, the two characteristic $–CH_2$ stretches of oleic acid were also significantly reduced, but the bands at 2922–2931 cm^{-1} noticeably increased from **MNPs-G1(Glu)** to **MNPs-G3(Glu)**.

Compared with FTIR spectra of L-glutamic acid dendrimers, such as **G3(Glu)** (Fig. 2I), the bands at ~1730 cm^{-1} were observed in the functionalized MNPs due to the carbonyl vibration in carboxyl groups. Two bands at around 1650 and 1540 cm^{-1} also represented the –CO–NH– bands. Similarly, strong Fe–O vibrations were observed at about 600 cm^{-1}. In both series of dendrimer-modified MNPs, the positions of the amide bands were shifted, probably resulting from conformational changes during the ligand-exchange process.

TGA measurement was employed to quantify the polypeptide dendritic ligands grafted onto the surface of the MNPs. For peptide dendritic ligands, the weight losses were only observed at one stage within the temperature range 150–450 °C. For example, the decomposition of dendritic ligands **G3(Lys)** and **G3 (Glu)** started at 285 °C and 295 °C, respectively, as shown in Fig. 3A and E. Fig. 3B–D and F–H show the weight losses of L-lysine- and L-glutamic acid-based dendritic ligands modified MNPs separately. The decomposition process was divided into three stages within the temperature range 35–1000 °C, which was similar to the initial oleic-acid-coated MNPs (Fig. 3I). The first stage was from 35 °C to 200 °C, within which the decrease in weight loss was below 10%. This is assigned to the evaporation of physically adsorbed water. The second weight loss step from 200 °C to 460 °C was attributed to the decomposition of the polypeptide dendritic ligands immobilized on the surfaces of MNPs. The TGA curves then suddenly leveled off in the third stage from 460 °C to 900 °C. This could be explained by the breaking of the covalent band between the Fe_3O_4 and dopamine.[50]

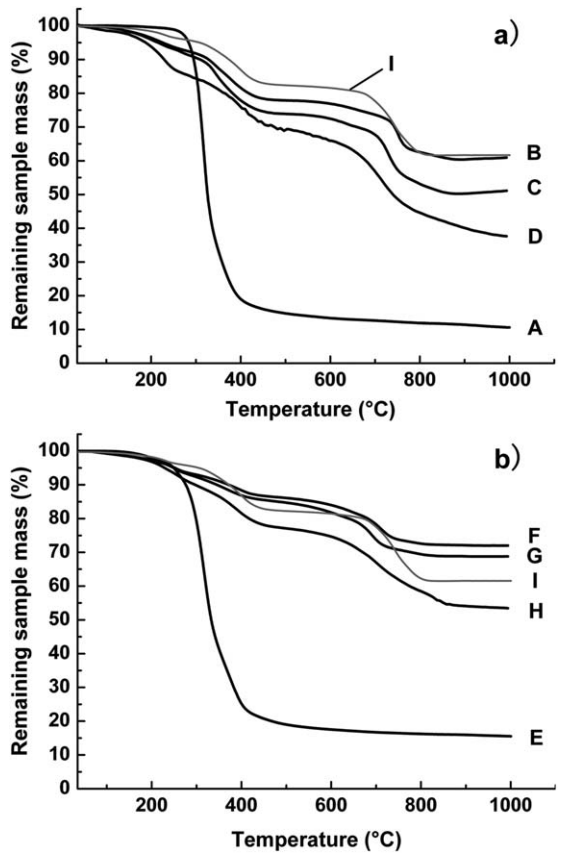

Fig. 3 TGA curves of polypeptide dendritic ligands and modified MNPs: (A) G3(Lys); (B) MNPs-G1(Lys); (C) MNPs-G2(Lys); (D) MNPs-G3(Lys); (E) G3(Glu); (F) MNPs-G1(Glu); (G) MNPs-G2(Glu); (H) MNPs-G3(Glu); (I) MNPs-OA.

The amount of polypeptide dendritic ligands covering the MNPs could be calculated using the TGA results. Table 1 summarizes the weight loss and the ligand coverage, which was calculated *via* the formula reported in the literature.[49] A similar phenomenon was observed in the MNPs modified with both L-lysine and L-glutamic acid dendrimers. The ligands per particle decreased with increasing generation due to the steric hindrance between the polypeptide dendritic ligands and the magnetic core in the ligand-exchange reaction, but the total amount of the terminal amino or carboxyl groups still increased with increasing generation. Therefore, the modification of higher-generation dendritic ligands introduced more well-organized functional groups on the surface, which could serve as anchor points for further attachment of biological molecules, such as target ligands, drugs or proteins, to achieve targeted delivery or specific biological functions.

Dispersibility and stability of the functionalized MNPs in water

The dispersibility and stability of the MNPs in water is very important for biological applications. Fig. 4 shows that **MNPs-OA** coated with a hydrophobic layer of oleic acid dissolved very well in *n*-hexane. After the ligand-exchange reaction, the hydrophilicity of particles greatly improved, enabling phase transfer. Both of L-lysine and L-glutamic acid dendritic ligands modified MNPs exhibited excellent water dispersibility due to the water soluble peptide dendrimers. No precipitates were observed even after one month. Moreover, the polypeptide dendrimers modified MNPs could be dispersed in various organic solvents to form stable magnetic colloids, such as ethanol, methanol and DMSO. This phenomenon should be partly ascribed to the amphiphilic peptide dendritic ligands, which are encouraging for the development of MNPs modified with biocompatible polypeptide dendrimers and their analogs as novel biomaterials.

Crystalline structure and size of the functionalized MNPs

The crystal structure of the MNPs was determined by XRD,[51,52] as shown in Fig. 5. The position and relative intensity of all diffraction signals matched well with the characteristic peaks of magnetite crystals obtained from standard Fe_3O_4 powder diffraction data.[13] The results revealed that the ligand-exchange reaction did not change the structure of the MNPs. The average crystallite sizes calculated from Scherrer's formula[53] were consistent with those measured by TEM, as shown in Table 1, though there was a little deviation. This could be ascribed to the different mechanism of the two techniques for the measurements of the particle sizes.

The morphology and size of the modified MNPs was determined by TEM. Fig. 6 shows the TEM micrographs of the MNPs before and after ligand-exchange with different generations of peptide dendritic ligands (**G1**–**G3**). The diameter and polydispersity calculated by averaging more than 50 MNPs are summarized in Table 1. The oleic-acid-stabilized MNPs were nearly spherical with an average size of 8.8 nm, as shown in Fig. 6A. Fig. 6B–G indicate that the peptide dendrimer-modified MNPs were nearly monodisperse in water after the phase

Table 1 The calculated numbers of ligands on each functionalized MNP (data were obtained from three independent experiments), and particle diameters and magnetic properties for the MNPs

	TGA				Size (nm)			M_s (emu g^{-1})	
Sample	Weight loss (ω%)	Ligands/particle	–NH_2 /particle	–COOH /particle	XRD	TEM	DLS	VSM	TGA[a]
MNPs-OA	35	—	—	—	9.03	8.82 ± 1.09	9.2 ± 1.8	44.8	—
MNPs-G1(Lys)	24.39	984	1968	—	12.49	9.62 ± 0.81	12.3 ± 3.8	53.4	52
MNPs-G2(Lys)	28.85	644	2576	—	9.25	9.49 ± 0.83	15.5 ± 4.3	50.3	49
MNPs-G3(Lys)	37.92	496	3968	—	10.43	9.74 ± 0.87	25.0 ± 8.5	41.6	42
MNPs-G1(Glu)	20.92	1083	—	2166	8.89	9.62 ± 1.20	13.4 ± 4.3	55.0	54
MNPs-G2(Glu)	24.31	569	—	2276	9.80	9.18 ± 0.97	16.1 ± 4.0	50.1	52
MNPs-G3(Glu)	30.31	367	—	2936	10.13	9.22 ± 0.94	26.2 ± 9.2	42.9	48

[a] Calculated from magnetic content determined *via* TGA in Table 1.

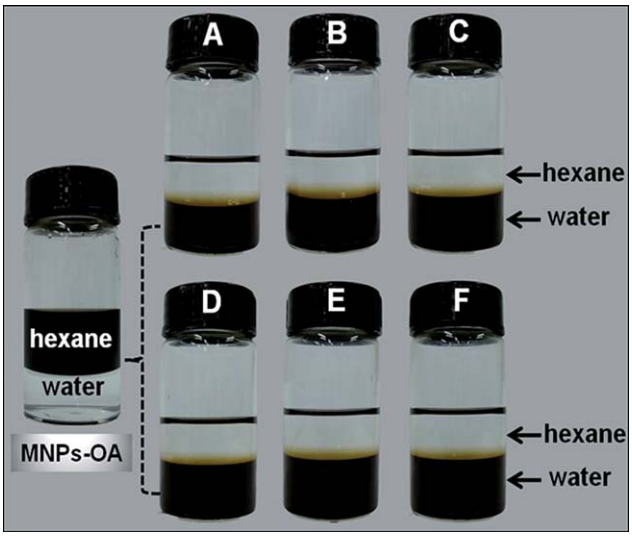

Fig. 4 The dispersibility of the functionalized MNPs varied from *n*-hexane to water. (A) MNPs-G1(Lys); (B) MNPs-G2(Lys); (C) MNPs-G3 (Lys); (D) MNPs-G1(Glu); (E) MNPs-G2(Glu); (F) MNPs-G3(Glu).

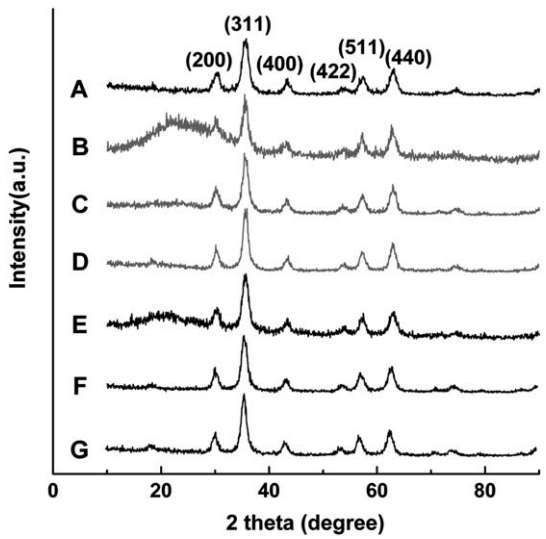

Fig. 5 XRD patterns of (A) MNPs-OA; (B) MNPs-G1(Lys); (C) MNPs-G2(Lys); (D) MNPs-G3(Lys); (E) MNPs-G1(Glu); (F) MNPs-G2(Glu); (G) MNPs-G3(Glu).

transfer. Compared with the TEM image of the initial MNPs, the morphology of the modified particles changed from sphere-like to cube-like, indicating slight Fe_3O_4 surface corrosion during the exchange. This phenomenon was in agreement with the previous report.[24] TEM measurement only provides the information for the inorganic ferrite core, since organic materials are transparent by TEM. Thus, the sizes for all the functionalized MNPs given in Table 1 are approximate.

DLS was used to determine the hydrodynamic diameter of the MNPs, including the peptide dendritic ligands coating and the ferric core. In Fig. 7, only one narrow peak in the size distribution was observed before and after ligand-exchange indicating excellent monodispersity. After modification, the hydrodynamic diameter of nanoparticles increased with the dendritic generations increasing, which were around 12.3, 15.5, 25.0 nm for the MNPs functionalized with **G1(Lys)**, **G2(Lys)**, **G3(Lys)** (Fig. 7a) and 13.4, 16.1, 26.2 nm for the ones with **G1(Glu)**, **G2(Glu)**, **G3 (Glu)** (Fig. 7b), respectively. Additionally, the size distribution of the modified MNPs became broader with the dendritic generation increasing. This phenomenon mainly attributed to increased molecular weight and size for higher generation,[35,36] and partly owing to the enhanced hydration properties resulting from more peripheral functional groups. The DLS measurement confirmed the feasibility to produce high quality ultrafine monodisperse MNPs with controllable sizes *via* peptide dendrimers. To our knowledge, this is the first synthesis of this kind of hydrophilic MNP with polypeptide dendrimers less than 30 nm in size by the ligand-exchange method. The ultra-small hydrodynamic diameter should be effective at overcoming biological defense systems and vascular barriers through enhanced permeability and retention (EPR) effects to the target tissues in the field of biomedicine.[22]

Magnetic properties of the MNPs

To study the magnetic behavior before and after the peptide dendritic ligand-exchange, VSM was employed to measure the magnetization (Fig. 8). The magnetization curve for oleic-acid-coated MNPs showed no hysteresis and was completely reversible at room temperature (Fig. 8A). Neither coercivity nor remanence was observed, indicating a typical superparamagnetic behavior.[9,47,49,50] After the ligand-exchange process, the hysteresis loops of the modified MNPs still past 0 Oe (Fig. 8B–G). Therefore the superparamagnetic properties were successfully

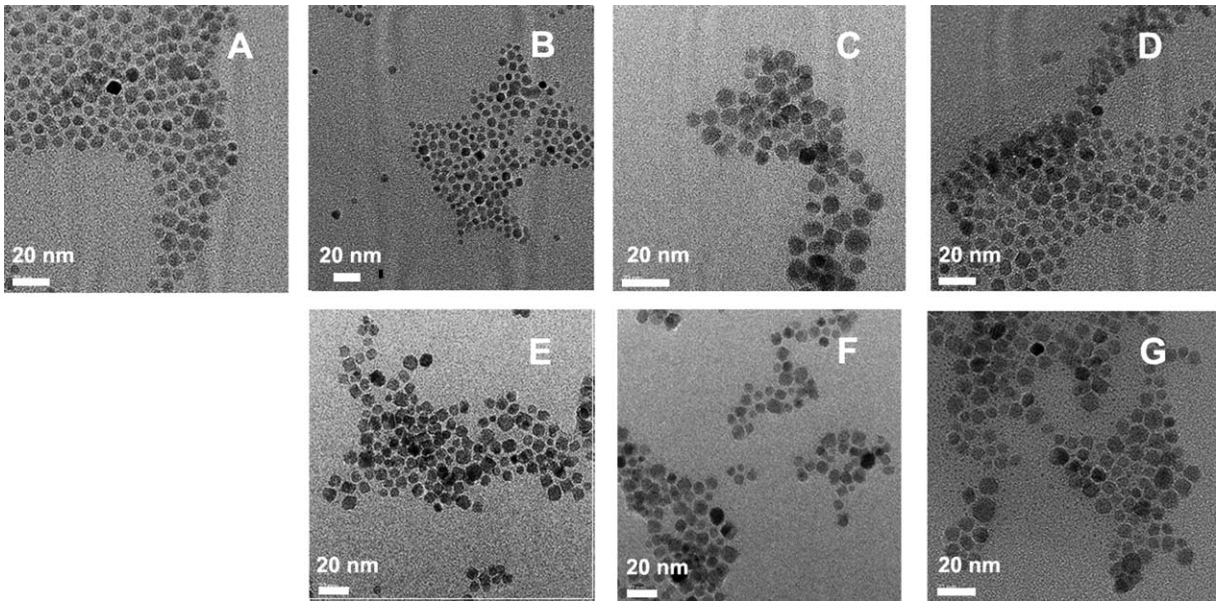

Fig. 6 TEM images of the MNPs: (A) MNPs-OA; (B) MNPs-G1(Lys); (C) MNPs-G2(Lys); (D) MNPs-G3(Lys); (E) MNPs-G1(Glu); (F) MNPs-G2 (Glu); (G) MNPs-G3(Glu). A was in *n*-hexane; B–G were in water.

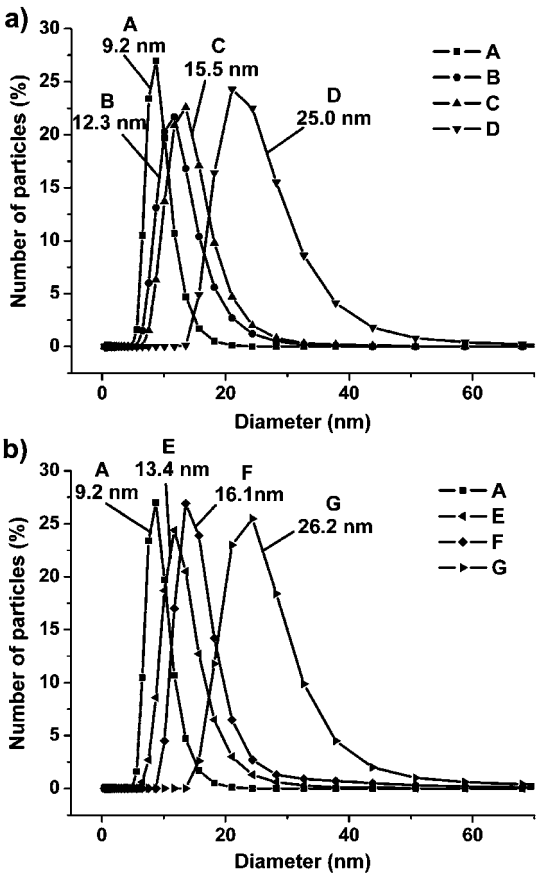

Fig. 7 The size distribution of the dendrimer-functionalized MNPs by DLS: (A) MNPs-OA; (B) MNPs-G1(Lys); (C) MNPs-G2(Lys); (D) MNPs-G3(Lys); (E) MNPs-G1(Glu); (F) MNPs-G2(Glu); (G) MNPs-G3(Glu).

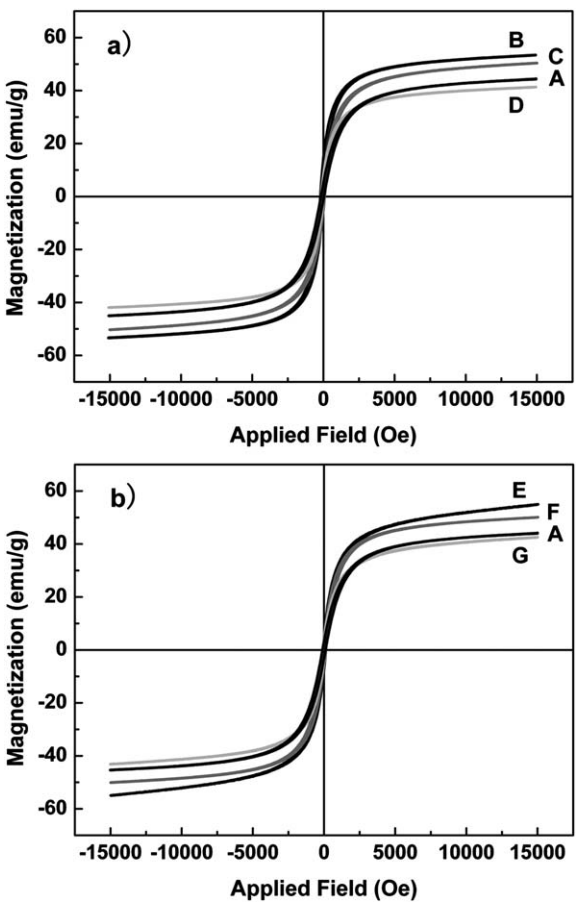

Fig. 8 Hysteresis loops for the MNPs at room temperature: (A) MNPs-OA; (B) MNPs-G1(Lys); (C) MNPs-G2(Lys); (D) MNPs-G3(Lys); (E) MNPs-G1(Glu); (F) MNPs-G2(Glu); (G) MNPs-G3(Glu).

retained and not affected by the introduction of different series of peptide dendritic ligands.

Table 1 summarizes the saturation magnetization (M_s) of the MNPs. For oleic-acid-coated MNPs, the saturation magnetization was ~44.8 emu g^{-1} (Fig. 8A). After the ligand-exchange reaction *via* L-lysine-based dendritic ligands (Fig. 8B–D), The saturation magnetization significantly increased to 53.4 emu g^{-1} for **MNPs-G1(Lys)** and decreased to 41.6 emu g^{-1} for **MNPs-G3(Lys)**. Similarly, for L-glutamic acid-functionalized MNPs (**G1**–**G3**), the saturation magnetization fell significantly from 55.0 to 42.9 emu g^{-1}. According to the previous studies, the saturation magnetization is in direct proportion to the particle size.[13] However, the two series of modified MNPs had extremely similar-sized iron cores, as observed in the TEM images in Fig. 6. The main reason for the variation of magnetization should therefore be ascribed to the introduction of a nonmagnetic mass onto the nanoparticles' surface and the different magnetic content per gram of particles (Table 1). The largest saturation magnetization for **G1(Glu)**-functionalized MNPs (55.0 emu g^{-1}) was ascribed to the lowest amount of organic compounds on each particle surface (20.92%). In contrast, a great loss of magnetization per gram of particles was observed when **G3(Lys)** and **G3(Glu)** were used for ligand-exchange because of the surface coverage of each particle increased to 37.92% and 30.31% separately. The M_s value could also be estimated on the basis of TGA data using eqn (1) (see also Table 1)[49] where $M_s^{MNPs\text{-}OA}$ is the saturation magnetization of oleic-acid-coated MNPs (44.8 emu g^{-1}) and ω is the mass loss (%) determined by TGA. The saturation magnetization values measured *via* VSM were consistent with those calculated by TGA.

$$M_s = \frac{M_s^{MNPs\text{-}OA}(1-\omega)}{1-\omega^{MNPs\text{-}OA}} \quad (1)$$

Surface charge of polypeptide dendritic ligands modified MNPs

The zeta potential provides an important parameter to determine the surface charge of nanoparticles and calculate the isoelectric point (pI). Fig. 9 shows a plot of the zeta potential *vs.* the pH for the two series of functionalized MNPs. In the case of MNPs modified with L-lysine-based dendrimers (Fig. 9A–C), the particles were positively charged under acidic conditions, with a surface potential higher than +30 mV at pH < 3. This can be attributed to the presence of amino groups on the particle surface, and those groups were in their protonated form.[54] The pIs of these MNPs were all at pH > 9, indicating the loss of protonated amino groups. Under such basic conditions, the abundant OH^- resulted in the surface being negatively charged. In contrast, the MNPs functionalized with L-glutamic acid dendrimers (Fig. 9 D–F) were negatively charged almost over the entire pH range due to the abundance of peripheral carboxyl groups. The pIs were observed at around pH = 3. Slight differences of pIs were also observed for both series of MNPs modified with different generations (**G1**–**G3**) of dendritic ligands, separately. It is noteworthy that all the functionalized MNPs tended to aggregate when the pH was close to the pI due to the small amount of electrostatic repulsion and the attractive van der Waals force. The MNPs modified with higher dendritic generations (**G3**) showed greater stability in aqueous solution than those modified with lower dendritic generations (**G1**) in both series, because of the steric interactions of dendritic ligands and the electrostatic repulsions. Similar steric interactions have also been observed in the case of PEG-modified MNPs.[49] For the MNPs modified with both L-lysine and L-glutamic acid dendrimers, no aggregation was observed in the pH range 2–9 and 5–12, respectively. This implies that the functionalized MNPs are potentially suitable for biomedical applications in different media.

Positively charged nanoparticles show a higher rate of cellular uptake by the phagocytic system compared with the neutral or negatively charged formulations.[55] Thus, the MNPs modified with L-lysine-based dendritic ligands might be available as multifunctional drugs or gene delivery carriers due to their positive charge.[7,39,56,57] On the other hand, the polypeptide dendrimers can also be utilized to functionalize other hydrophobic nanoparticles, such as quantum dots or Au nanoparticles, merely by altering the connecting ligands. The biomedical applications of nanoparticles functionalized with polypeptide dendritic ligands are currently being explored in our group.

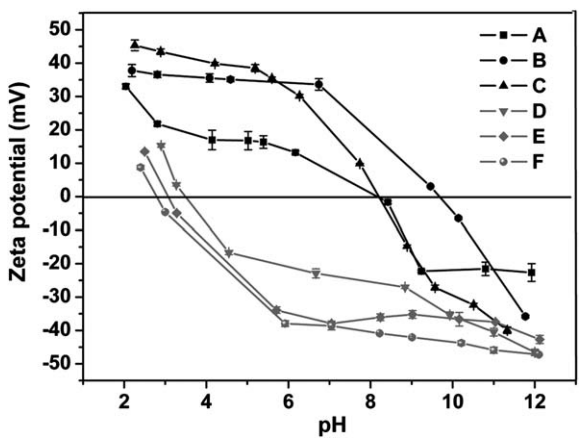

Fig. 9 Zeta potential *vs.* pH of dendrimer-functionalized MNPs: (A) MNPs-G1(Lys); (B) MNPs-G2(Lys); (C) MNPs-G3(Lys); (D) MNPs-G1(Glu); (E) MNPs-G2(Glu); (F) MNPs-G3(Glu).

Conclusions

In this paper, a new family of MNPs surface-functionalized with polypeptide dendrimers were successfully designed and fabricated by the ligand-exchange method without changing the crystalline structure. Two series of MNPs modified with L-lysine and L-glutamic acid dendrimers showed controllable peripheral functional groups, excellent dispersibility and long-term colloidal stability in aqueous solution over a broad pH range. The hydrodynamic diameters of the functionalized MNPs were all less than 30 nm and increased gradually with increasing generation. The superparamagnetism of the MNPs was not affected by the ligand-exchange process. Modified MNPs with the same generation number of peptide dendritic ligands exhibited similar magnetization. **MNPs-G1(Lys)** and **MNPs-G1(Glu)** possessed the largest saturation magnetization values, 53.4 and 55.0 emu g^{-1} in their respective series, which is larger than the oleic-acid-coated MNPs. The saturation magnetization of modified MNPs reduced from ~55 to ~42 emu g^{-1} with increasing dendritic generation because of an increased nonmagnetic mass on the surface. The peptide dendritic ligands not only afforded phase-transferred MNPs high water-solubility, but could also

serve as potential anchor points for the attachment of biological molecules. Their functionalization with peptide dendrimers to achieve the synthesis of high quality MNPs provides a unique approach to design and explore new nanobiomaterials.

Acknowledgements

The authors thank P. C. Deng, X. M. Jia and X. Y. Wang (Analytical & Testing Center, Sichuan University) for testing samples in NMR. This research work was supported by the National Basic Research Program of China (National 973 program, No. 2011CB606206), the National Natural Science Foundation of China (31070849, 50830105), the Department of Science and Technology of Sichuan Province (2009HH0001) and the Ministry of Science and Technology (2010DFA51550).

References

1 S. Hanessian, J. A. Grzyb, F. Cengelli and L. Juillerat-Jeanneret, *Bioorg. Med. Chem.*, 2008, **16**, 2921–2931.
2 M. K. Yu, Y. Y. Jeong, J. Park, S. Park, J. W. Kim, J. J. Min, K. Kim and S. Jon, *Angew. Chem., Int. Ed.*, 2008, **47**, 5362–5365.
3 R. R. Qiao, C. H. Yang and M. Y. Gao, *J. Mater. Chem.*, 2009, **19**, 9286–9286.
4 C. Fang and M. Q. Zhang, *J. Mater. Chem.*, 2009, **19**, 6258–6266.
5 M. Zanella, A. Falqui, S. Kudera, L. Manna, M. F. Casula and W. J. Parak, *J. Mater. Chem.*, 2008, **18**, 4311–4317.
6 S. Mornet, S. Vasseur, F. Grasset, P. Veverka, G. Goglio, A. Demourgues, J. Portier, E. Pollert and E. Duguet, *Prog. Solid State Chem.*, 2006, **34**, 237–247.
7 B. F. Pan, D. X. Cui, Y. Sheng, C. G. Ozkan, F. Gao, R. He, Q. Li, P. Xu and T. Huang, *Cancer Res.*, 2007, **67**, 8156–8163.
8 J. Kim, Y. Piao, N. Lee, Y. Il Park, I. H. Lee, J. H. Lee, S. R. Paik and T. Hyeon, *Adv. Mater.*, 2010, **22**, 57–60.
9 J. Liu, Z. K. Sun, Y. H. Deng, Y. Zou, C. Y. Li, X. H. Guo, L. Q. Xiong, Y. Gao, F. Y. Li and D. Y. Zhao, *Angew. Chem., Int. Ed.*, 2009, **48**, 5875–5879.
10 Y. Deng, D. Qi, C. Deng, X. Zhang and D. Zhao, *J. Am. Chem. Soc.*, 2008, **130**, 28–29.
11 J. Liu, Z. Sun, Y. Deng, Y. Zou, C. Li, X. Guo, L. Xiong, Y. Gao, F. Li and D. Zhao, *Angew. Chem.*, 2009, **121**, 5989–5993.
12 Y. Deng, C. Deng, D. Qi, C. Liu, J. Liu, X. Zhang and D. Zhao, *Adv. Mater.*, 2009, **21**, 1377–1382.
13 S. H. Sun, H. Zeng, D. B. Robinson, S. Raoux, P. M. Rice, S. X. Wang and G. X. Li, *J. Am. Chem. Soc.*, 2004, **126**, 273–279.
14 S. J. Park, S. Kim, S. Lee, Z. G. Khim, K. Char and T. Hyeon, *J. Am. Chem. Soc.*, 2000, **122**, 8581–8582.
15 K. Woo, J. Hong, S. Choi, H. W. Lee, J. P. Ahn, C. S. Kim and S. W. Lee, *Chem. Mater.*, 2004, **16**, 2814–2818.
16 H. Lee, E. Lee, D. K. Kim, N. K. Jang, Y. Y. Jeong and S. Jon, *J. Am. Chem. Soc.*, 2006, **128**, 7383–7389.
17 I. Robinson, C. Alexander, L. T. Lu, L. D. Tung, D. G. Fernig and N. T. K. Thanh, *Chem. Commun.*, 2007, 4602–4604.
18 C. J. Xu and S. H. Sun, *Polym. Int.*, 2007, **56**, 821–826.
19 J. Qin, S. Laurent, Y. S. Jo, A. Roch, M. Mikhaylova, Z. M. Bhujwalla, R. N. Muller and M. Muhammed, *Adv. Mater.*, 2007, **19**, 2411–2411.
20 J. F. Berret, N. Schonbeck, F. Gazeau, D. El Kharrat, O. Sandre, A. Vacher and M. Airiau, *J. Am. Chem. Soc.*, 2006, **128**, 1755–1761.
21 B. S. Kim, J. M. Qiu, J. P. Wang and T. A. Taton, *Nano Lett.*, 2005, **5**, 1987–1991.
22 Y. W. Jun, J. H. Lee and J. Cheon, *Angew. Chem., Int. Ed.*, 2008, **47**, 5122–5135.
23 T. R. Zhang, J. P. Ge, Y. P. Hu and Y. D. Yin, *Nano Lett.*, 2007, **7**, 3203–3207.
24 J. Xie, C. J. Xu, Z. H. Xu, Y. L. Hou, K. L. L. Young, S. X. Wang, N. Pourmand and S. H. Sun, *Chem. Mater.*, 2007, **19**, 1202–1202.
25 H. B. Liu, J. Guo, L. Jin, W. L. Yang and C. C. Wang, *J. Phys. Chem. B*, 2008, **112**, 3315–3321.
26 K. L. Young, C. J. Xu, J. Xie and S. H. Sun, *J. Mater. Chem.*, 2009, **19**, 6400–6406.
27 J. Qin, Y. S. Jo and M. Muhammed, *Angew. Chem., Int. Ed.*, 2009, **48**, 7845–7849.
28 M. Talelli, C. J. F. Rijcken, T. Lammers, P. R. Seevinck, G. Storm, C. F. van Nostrum and W. E. Hennink, *Langmuir*, 2009, **25**, 2060–2067.
29 T. J. Daou, G. Pourroy, J. M. Greneche, A. Bertin, D. Felder-Flesch and S. Begin-Colin, *Dalton Trans.*, 2009, 4442–4449.
30 M. Kim, Y. F. Chen, Y. C. Liu and X. G. Peng, *Adv. Mater.*, 2005, **17**, 1429–1430.
31 M. H. Park, Y. Ofir, B. Samanta and V. M. Rotello, *Adv. Mater.*, 2009, **21**, 2323.
32 N. Malik, R. Wiwattanapatapee, R. Klopsch, K. Lorenz, H. Frey, J. W. Weener, E. W. Meijer, W. Paulus and R. Duncan, *J. Controlled Release*, 2000, **65**, 133–148.
33 R. Jevprasesphant, J. Penny, D. Attwood, N. B. McKeown and A. D'Emanuele, *Pharm. Res.*, 2003, **20**, 1543–1550.
34 J. H. S. Kuo, M. S. Jan and H. W. Chu, *J. Pharm. Pharmacol.*, 2005, **57**, 489–495.
35 L. Crespo, G. Sanclimens, M. Pons, E. Giralt, M. Royo and F. Albericio, *Chem. Rev.*, 2005, **105**, 1663–1681.
36 S. H. Medina and M. E. H. El-Sayed, *Chem. Rev.*, 2009, **109**, 3141–3157.
37 K. Luo, C. X. Li, G. Wang, Y. Nie, B. He, Y. Wu and Z. W. Gu, *J. Controlled Release*, 2010, DOI: 10.1016/j.jconrel.2010.10.006.
38 K. Luo, G. Liu, X. W. Zhang, W. C. She, B. He, Y. Nie, L. Li, Y. Wu, Z. R. Zhang, Q. Y. Gong, F. B. Gao, B. Song, H. Ai and Z. W. Gu, *Macromol. Biosci.*, 2009, **9**, 1227–1236.
39 H. Yuan, K. Luo, Y. S. Lai, Y. J. Pu, B. He, G. Wang, Y. Wu and Z. W. Gu, *Mol. Pharmaceutics*, 2010, **7**, 953–962.
40 K. Luo, G. Liu, B. He, Y. Wu, Q. Y. Gong, B. Song, H. Ai and Z. W. Gu, *Biomaterials*, 2011, **32**, 2575–2585.
41 C. J. Xu, K. M. Xu, H. W. Gu, R. K. Zheng, H. Liu, X. X. Zhang, Z. H. Guo and B. Xu, *J. Am. Chem. Soc.*, 2004, **126**, 9938–9939.
42 Y. Li, Q. B. Li, F. X. Li, H. Y. Zhang, L. Jia, J. Y. Yu, Q. Fang and A. Cao, *Biomacromolecules*, 2006, **7**, 224–231.
43 F. E. Appoh, D. S. Thomas and H. B. Kraatz, *Macromolecules*, 2005, **38**, 7562–7570.
44 Y. M. Huh, Y. W. Jun, H. T. Song, S. Kim, J. S. Choi, J. H. Lee, S. Yoon, K. S. Kim, J. S. Shin, J. S. Suh and J. Cheon, *J. Am. Chem. Soc.*, 2005, **127**, 12387–12391.
45 M. A. White, J. A. Johnson, J. T. Koberstein and N. J. Turro, *J. Am. Chem. Soc.*, 2006, **128**, 11356–11357.
46 D. B. Robinson, H. H. J. Persson, H. Zeng, G. X. Li, N. Pourmand, S. H. Sun and S. X. Wang, *Langmuir*, 2005, **21**, 3096–3103.
47 D. K. Nagesha, B. D. Plouffe, M. Phan, L. H. Lewis, S. Sridhar and S. K. Murthy, *J. Appl. Phys.*, 2009, **105**, 07B317.
48 K. Heuze, D. Rosario-Amorin, S. Nlate, M. Gaboyard, A. Boutercd and R. Clerac, *New J. Chem.*, 2008, **32**, 383–387.
49 R. De Palma, S. Peeters, M. J. Van Bael, H. Van den Rul, K. Bonroy, W. Laureyn, J. Mullens, G. Borghs and G. Maes, *Chem. Mater.*, 2007, **19**, 1821–1831.
50 W. H. Zhou, C. H. Lu, X. C. Guo, F. R. Chen, H. H. Yang and X. R. Wang, *J. Mater. Chem.*, 2010, **20**, 880–883.
51 Y. H. Deng, Y. Cai, Z. K. Sun, J. Liu, C. Liu, J. Wei, W. Li, C. Liu, Y. Wang and D. Y. Zhao, *J. Am. Chem. Soc.*, 2010, **132**, 8466–8473.
52 Y. H. Deng, C. C. Wang, J. H. Hu, W. L. Yang and S. K. Fu, *Colloids Surf., A*, 2005, **262**, 87–93.
53 Q. Zhang, C. H. Wang, L. Qiao, H. S. Yan and K. L. Liu, *J. Mater. Chem.*, 2009, **19**, 8393–8402.
54 A. Lopez-Cruz, C. Barrera, V. L. Calero-DdelC and C. Rinaldi, *J. Mater. Chem.*, 2009, **19**, 6870–6876.
55 F. Alexis, E. Pridgen, L. K. Molnar and O. C. Farokhzad, *Mol. Pharmaceutics*, 2008, **5**, 505–515.
56 Y. Zhang, J. Y. Liu, F. Yang, Y. J. Zhang, Q. Yao, T. Y. Cui, X. Zhao and Z. D. Zhang, *J. Mater. Sci.: Mater. Med.*, 2009, **20**, 2433–2440.
57 A. Bielinska, J. F. KukowskaLatallo, J. Johnson, D. A. Tomalia and J. R. Baker, *Nucleic Acids Res.*, 1996, **24**, 2176–2182.

